molecular pharmaceutics

articles

Validation of In Vitro Cell-Based Human Blood−Brain Barrier Model Using Clinical Positron Emission Tomography Radioligands To Predict In Vivo Human Brain Penetration

Aloïse Mabondzo,*,† Michel Bottlaender,‡ Anne-Cécile Guyot,† Katya Tsaouin,§ Jean Robert Deverre,‡ and Praveen V. Balimane*,||

CEA, DSV, iBiTec-S, Service de Pharmacologie et d'Immunoanalyse, Gif-sur-Yvette, France, CEA, DSV, I2BM, Service Hospitalier Frédéric Joliot, Orsay, France, APREDICA, Watertown, Massachusetts, and Bristol-Myers Squibb Company, Princeton, New Jersey

Received May 13, 2010; Accepted August 26, 2010

Abstract: We have evaluated a novel in vitro cell-based human blood−brain barrier (BBB) model that could predict in vivo human brain penetration for compounds with different BBB permeabilities using the clinical positron emission tomography (PET) data. Comparison studies were also performed to demonstrate that the in vitro cell-based human BBB model resulted in better predictivity over the traditional permeability model in discovery organizations, Caco-2 cells. We evaluated the in vivo BBB permeability of [^{18}F] and [^{11}C]-compounds in humans by PET imaging. The in vivo plasma−brain exchange parameters used for comparison were determined in humans by PET using a kinetic analysis of the radiotracer binding. For each radiotracer, the parameters were determined by fitting the brain kinetics of the radiotracer using a two-tissue compartment model of the ligand−receptor interaction. Bidirectional transport studies with the same compounds as in in vivo studies were carried out using the in vitro cell-based human BBB model as well as Caco-2 cells. The in vitro cell-based human BBB model has important features of the BBB in vivo and is suitable for discriminating between CNS and non-CNS marketed drugs. A very good correlation ($r^2 = 0.90$; $P < 0.001$) was demonstrated between in vitro BBB permeability and in vivo permeability coefficient. In contrast, a poor correlation ($r^2 = 0.17$) was obtained between Caco-2 data and in vivo human brain penetration. This study highlights the potential of this in vitro cell-based human BBB model in drug discovery and shows that it can be an extremely effective screening tool for CNS programs.

Keywords: Drug transport study; human blood−brain barrier; in vivo−in vitro correlation; positron emission tomography

Introduction

Drug discovery and development in the pharmaceutical Industry is an extremely costly endeavor plagued by very high risk due to the high attrition rate in various stages of development. A recent report has put the total cost of bringing a drug to the market at greater than a billion dollars, with an average development time of twelve years.[1] Despite the considerable financial and resource investments, the number of drug approvals per year has remained steady, or even decreased, in the recent past. The advent of combinatorial chemistry, automation and high-throughput screening (HTS) has afforded the opportunity to test thousands of compounds, but the success rate in progressing from initial clinical testing to final approval has remained disappointingly low. Around 90% of the compounds entering phase I clinical testing fail to reach patients and as high as 50% entering phase III do not make the cut.[2] The situation seems to be even worse for drugs targeting the central nervous system

* Corresponding authors. A.M.: iBiTec-S/Service de Pharmacologie et d'Immunoanalyse, iBiTec-S/Service de Pharmacologie et d'Immunoanalyse, 91191 Gif sur Yvette Cedex, France; phone, (33-1) 69 08 13 21; fax, (33-1) 69 08 59 07; e-mail, Aloise.Mabondzo@cea.fr. P.V.B.: Bristol-Myers Squibb Company, Princeton, NJ 08543; phone, 609 252 4401; e-mail, Praveen.Balimane@bms.com.

† CEA, DSV, iBiTec-S, Service de Pharmacologie et d'Immunoanalyse.

‡ CEA, DSV, I2BM, Service Hospitalier Frédéric Joliot.

§ APREDICA.

|| Bristol-Myers Squibb Company.

(1) *Food and Drug Administration. Challenges and Opportunity on the critical path to new medical products*; FDA Report; FDA: Rockville, MD, 2004.

(2) Kola, I.; Landis, J. Can pharmaceutical industry reduce attrition rates? *Nat. Rev. Drug Discovery.* **2004**, *3*, 711–715.

10.1021/mp1002366
Published on Web 08/26/2010

(CNS), for which the success rate from first-in-man to registration could be only ~8% and is significantly lower than for other indications, such as cardiovascular, infectious, inflammatory, and metabolic diseases.[3] The development of drugs targeting the CNS requires precise knowledge of their brain penetration, and ideally, this information should be obtained as early as possible to avoid failure in late clinical development, when upward of $100 million is typically invested in a drug candidate. The physical transport and metabolic blood−brain barrier (BBB) is highly complex, and numerous in vitro models have been designed to study kinetic parameters in the CNS. These in vitro models include artificial membrane systems (PAMPA), noncerebral peripheral endothelial cell lines, immortalized rat brain endothelial cells, primary cultured bovine, porcine or rat brain capillary endothelial cells and cocultures of primary brain capillary cells with astrocytes.[4−10] In vitro BBB models must be carefully assessed for their capacity to reflect accurately the passage of drugs into the CNS in vivo. Currently, there is a significant unmet need for a predictive in vitro BBB model that could be used for assessing the brain penetration of CNS-targeted discovery compounds. We previously evaluated the BBB permeabilities of a series of compounds studied in vitro using a human BBB coculture system and in vivo with quantitative PET imaging in rats.[11] The objective was to investigate the ability of the novel in vitro BBB model to predict in vivo brain penetration in humans of drugs of different molecular size ranges and different BBB permeabilities. Due to the lack of a good predictive tool, several strategies combine in silico, in vivo and in vitro approaches. These normally include PAMPA, efflux ratio, and protein-binding properties to assess brain entry or in vivo brain-to-plasma ratio assessment in rodent models. These models are either not fully validated or very time-, cost- and resource-intensive. This creates a need for more appropriate screening methods that are predictive of the in vivo behavior of drugs in humans and which are relatively low cost and amenable to medium-throughput application in early/mid stage drug discovery programs.

Here we report for the first time the use of the in vitro human BBB model to study human BBB permeabilities of drugs, using PET to assess the predictive power of the in vitro cell-based BBB model and establish its utility as a screening tool in drug discovery and development.

Materials and Methods

Investigations and Research Using Human Subjects. For all the studies performed in our laboratory and more particularly studies concerning [^{11}C]flumazenil, [^{11}C]raclopride, [^{18}F]fluoro-A-85380, [^{18}F]-FDOPA and [^{11}C]befloxatone, the protocol was approved by a medical Bioethics Committee of Ile-de-France. Subjects gave their written informed consent after receiving an explanation of the study. This is indicated in the concerned papers. In the case of [^{11}C]-befloxatone (unpublished data), the protocol was approved by the Bioethics Committee "Ile-de-France-VII". Data for [^{18}F]-FDG are from the literature.

Labeled and Unlabeled Compounds. [U-^{14}C]Sucrose (601 mCi mmol^{-1}), [^{3}H]vinblastin (10.3 Ci mmol^{-1}) and [^{3}H]digoxin (37 mCi mmol^{-1}) were from Amersham (Buckinghamshire, U.K.); [^{3}H]haloperidol (12 Ci mmol^{-1}) and [^{3}H]propranolol (24.3 Ci mmol^{-1}) were from Perkin-Elmer; [^{3}H]etoposide (5 Ci mmol^{-1}) and taurocholic acid (10 Ci mmol^{-1}) were from ARC; [^{18}F]fluorodesoxyglucose ([^{18}F]-FDG) was from CIS bio (Saclay, France). The other compounds were radiolabeled as previously described: ([^{18}F]fluoro-Dopa, 2-[^{18}F]fluoro-A-85380,[12] [^{11}C]raclopride,[13] [^{11}C]flu-

(3) Hurko, O.; Ryan, J. L. Translational research in central nervous system drug discovery. *NeuroRx* **2005**, *2*, 671–682.
(4) Megard, I.; Garrigues, A.; Orlowski, S.; Jorajuria, S.; Clayette, P.; Ezan, E.; Mabondzo, A. A coculture-based model of human blood−brain barrier: application to active transport of indinavir and *in vivo-in vitro* correlation. *Brain Res.* **2002**, *927*, 153–167.
(5) Deli, M. A.; Abraham, C. S.; Kataoka, Y.; Niwa, M. Permeability studies on in vitro blood−brain barrier models: physiology, pathology and pharmacology. *Cell Mol Neurobiol.* **2005**, *25*, 59–120.
(6) Deli, M. A.; Joo, F. Cultured vascular endothelial cells of the brain. *Keio J. Med.* **1996**, *45*, 183–99.
(7) Begley, D. J.; Lechardeur, D.; Chen, Z. D.; Rollinson, C.; Bardoul, M.; Roux, F.; Scherman, D.; Abbott, N. J. Functional expression of P-glycoprotein in an immortalised cell line of rat brain endothelial cells, RBE4. *J. Neurochem.* **1996**, *67*, 988–995.
(8) Nakagawa, S.; Deli, M. A.; Kawaguchi, H.; Shimizudani, T.; Shimono, T.; Kittel, A.; Tanaka, K.; Niwa, M. A new blood−brain barrier model using primary rat brain endothelial cells, pericytes and astrocytes. *Neurochem. Int.* **2009**, *54*, 253–263.
(9) Zhang, Y.; Li, C. S.; Ye, Y.; Johnson, K.; Poe, J.; Johnson, S.; Bobrowski, W.; Garrido, R.; Madhu, C. Porcine brain microvessel endothelial cells as an in vitro model to predict in vivo blood−brain barrier permeability. *Drug Metab. Dispos.* **2006**, *34*, 1935–1943.
(10) Weksler, B. B.; Subileau, E. A.; Perrière, N.; Charneau, P.; Holloway, K.; Leveque, M.; Tricoire-Leignel, H.; Nicotra, A.; Bourdoulous, S.; Turowski, P.; Male, D. K.; Roux, F.; Greenwood, J.; Romero, I. A.; Couraud, P. O. Blood−brain barrier-specific properties of a human adult brain endothelial cell line. *FASEB J.* **2005**, *19*, 1872–1874.
(11) Josserand, V.; Pelerin, H.; de Bruin, B.; Jego, B.; Kuhnast, B.; Hinnen, F.; Duconge, F.; Boisgard, R.; Beuvon, F.; Chassoux, F.; Daumas-Duport, C.; Ezan, E.; Dolle, F.; Mabondzo, A.; Tavitian, B. Evaluation of drug penetration into the brain: a double study by in vivo imaging with positron emission tomography and using an in vitro model of the human blood−brain barrier. *J. Pharmacol. Exp. Ther.* **2006**, *316*, 79–86.
(12) Dolle, F.; Dolci, L.; Valette, H.; Hinnen, F.; Vaufrey, F.; Guenther, I.; Fuseau, C.; Coulon, C.; Bottlaender, M.; Crouzel, C. Synthesis and nicotinic acetylcholine receptor in vivo binding properties of 2-fluoro-3-[2(S)-2-azetidinylmethoxy]pyridine: a new positron emission tomography ligand for nicotinic receptors. *J. Med. Chem.* **1999**, *42*, 2251–2259.
(13) Langer, O.; Någren, K.; Dollé, F.; Lundkvist, C.; Sandell, J.; Swahn, C.-G.; et al. Precursor synthesis and radiolabelling of the dopamine D_2 receptor ligand [^{11}C]raclopride from [^{11}C]methyl triflate. *J. Labelled Compd. Radiopharm.* **1999**, *42*, 1183–1193.

mazenil,[14] [^{11}C]befloxatone.[15] [^{11}C]-PE2I,[16] [^{3}D]glucuronide-acetaminophen and [^{13}C]-1-hydroxymidazolam and rosuvastatin were from Toronto Research Chemicals (North York, Canada). The following nonradiolabeled compounds, acetaminophen, midazolam, rosuvastatin, dextrometorphan and caffeine, were also used as reference set for establishment of dynamic range of in vitro cell-based human BBB permeability. Acetaminophen, midazolam, dextromethorphan, were purchased from Sigma-Aldrich (St. Louis, MO); caffeine was obtained from Fluka-Sigma Aldrich. Internal standards (meloxicam, lansoprazole, levallorphan) for tandem liquid chromatography mass spectrometry (LC/MS/MS) analysis were purchased from Sigma-Aldrich.

Diagram of the Experimental Setup Highlighting the Architecture of the Cell-Based Human BBB Model. *Isolation of Human Brain Endothelial Cells and Astrocytes.* Normal appearing human adult brain tissues were obtained from patients undergoing surgery for epilepsy. The neurosurgeons provided samples of brain cortex located as far as possible from the epileptogenic lesion. The samples were considered to be healthy tissue on the basis of neuroimaging. Cells were isolated from brain samples after 1.5 h digestion with collagenase/Dispase (1 mg/mL, Roche, France) containing DNase 1 (20 units/mL, Roche, France), followed by a 20% BSA gradient as described elsewhere.[6] The resulting microvessels obtained in the pellet were further digested with collagenase-Dispase (1 mg/mL, Roche, France) containing DNase 1 (20 units/mL, Roche, France) for 1 h at 37 °C while the supernatant containing a layer of myelin was centrifuged, washed and cultured in 75 cm^2 in the astrocyte specific medium supplemented with 10 μg mL^{-1} hEGF, 10 mg mL^{-1} insulin, 25 μg mL^{-1} progesterone, 50 mg mL^{-1} transferrin, 50 mg mL^{-1} gentamicin, 50 μg mL$^{-1\%}$ amphotericin-B, 1% of human serum and 5% of fetal bovine serum to generate pure astrocytes. The purity of astrocytes was checked by immunostaining for glial fibrillary acidic protein (GFAP).

Microvessel endothelial cells clusters after collagenase-Dispase digestion, were passed through a 20 μm nylon mesh. The microvessels retained by the nylon mesh were collected and washed twice in endothelial basal medium before plating in 25 cm^2 flask cultured coated with collagen type IV and fibronectin (0.1 mg/mL) in the presence of puromycine (2 μg/mL) in the endothelial basal medium containing 0.1% human recombinant epidermal growth factor (hEGF), 0.04% hydrocortisone, 0.1% human recombinat insuline like growth factor, 0.1% ascorbic acid, 0.1% gentamin, 0.1% amphotericin-BN and 5% fetal bovine serum. On the third day, the cells received a new endothelial specific medium without puromycine. When cells reached confluence (70%) at day 7, the purified endothelial cells were frozen and ready to be used for in vitro cell-based human BBB genesis and drug transport experiments.

Cell-Based Human Blood−Brain Barrier Model. The model, previously described, consisted of a monolayer of primary adult human brain endothelial cells (BECs) and primary adult human astrocytes from the same individual.[4] Briefly, human astrocytes (2×10^4 cells) were plated on Transwell^R plates (Costar, Dutscher SA, Brumath, France) in an the astrocyte specific medium (α-MEM/F12) supplemented with 10 μg mL^{-1}, hEGF, 10 mg mL^{-1}insulin, 25 μg mL^{-1} progesterone, 50 mg mL^{-1} transferrin, 50 mg mL^{-1} gentamicin, 50 μg mL$^{-1\%}$ amphotericin-B, 1% of human serum and 5% of fetal bovine serum. After 24−72 h, BECs (5×10^4 cells) were plated on the upper side of a collagen-coated polyester Transwell^R membrane (Costar, pore size 0.4 μm; diameter 12 mm; insert growth area 1 cm^2) in 0.5 mL of the endothelial basal medium-2 (EBM-2, LONZA, Walkersville, MD) containing 0.1% human recombinant epidermal growth factor (hEGF), 0.04% hydrocortisone, 0.1% human recombinat insuline like growth factor, 0.1% ascorbic acid, 0.1% gentamin, 0.1% amphotericin-BN and 5% fetal bovine serum. (0.5 mL). The chambers containing human astrocytes and BECs were considered as the basolateral and apical compartment, respectively. The microplates were then incubated at 37 °C in a 5% CO_2 atmosphere. Under these experimental conditions, BECs formed a confluent monolayer within 15 days (Figure 1).

Functional Evaluation of In Vitro Cell-Based Human BBB Model. *Evidence of Efflux Transporters.* For a thorough evaluation of the in vitro BBB model, the mRNA expression profiles of ABC transporters (ABCB1, ABCC1, ABCC2, ABCC4, ABCC6, ABCG2), and claudin-3, claudin-5 and ZO-1 were assessed as previously described.[17] RNA was isolated using GenElute mammalian total RNA kit (Sigma, Aldrich). Total RNA concentration and purity were then determined by measuring absorbance at 260 and 280 nm. The A260/280 ratio ranged between 1.8 and 2. A sample of 0.5 μg of total RNA was converted to cDNA with random primers in a total volume of 10 μL using RT^2 first strand kit (Superarray Bioscience Corporation, USA). The cDNA was diluted with distilled water to a volume of 100 μL. 0.4 μM was used for each primer set in a specific RT^2 profiler PCR array according to the manufacturer's protocol. Relative expression values were calculated as $2^{-\Delta CT}$, where ΔCT is the difference of the amplification curve (CT) values for genes of interest and the housekeeping gene (hypoxanthine-guanine phosphoribosyltransferase, HPRT). If the CT was

(14) Mazière, M.; Hantraye, P.; Prenant, C.; Sastre, J.; Comar, D. Synthesis of ethyl 8-fluoro-5,6-dihydro-5-(11C)methyl-6-oxo-4H-imidazo (1,5-a) benzodiazepine-3-carboxylate (Ro 15-1788): a specific radioligan for in vivo study of central benzodiazepine receptors by positron emission tomography. *Int. J. Appl. Radiat. Isot.* **1984**, *35*, 973–978.

(15) Dolle, F.; Valette, H.; Bramoulle, Y.; Guenther, I.; Fuseau, C.; Coulon, C.; Lartizien, C.; Jegham, S.; George, P.; Curet, O.; Pinquier, J. L.; Bottlaender, M. Synthesis and in vivo imaging properties of [11C]befloxatone: a novel highly potent positron emission tomography ligand for mono-amine oxydase-A. *Bioorg. Med. Chem. Lett.* **2003**, *13*, 1771–1775.

(16) Dollé, F.; Bottlaender, M.; Demphel, S.; Emond, P.; Fuseau, C.; Coulon, C.; Ottaviani, M.; Valette, H.; Loc'h, Halldin, C.; Mauclaire, L.; Guilloteau, D.; Mazière, B.; Crouzel, C. High efficient synthesis of [11C]PE2I, a selective radioligand for the quantification of the dopamine transporter using PET. *J. Labelled Compd Radiopharm.* **2000**, *43*, 997–1004.

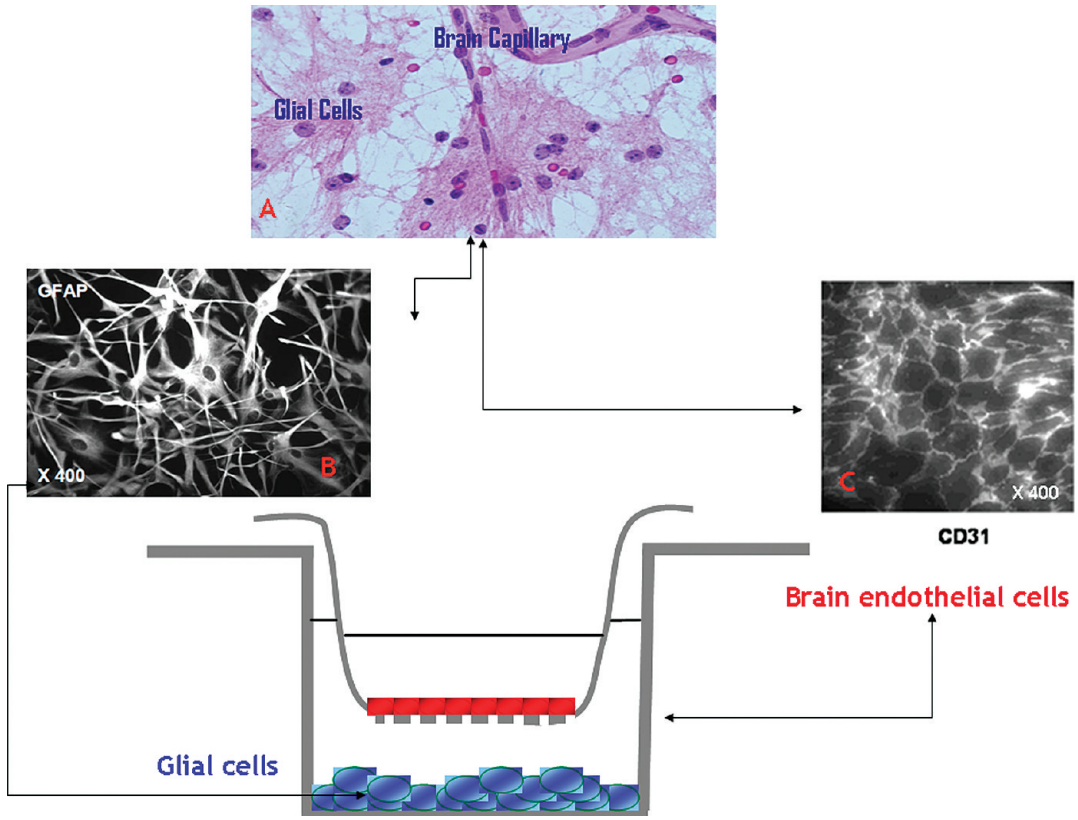

Figure 1. Diagram of the experimental setup highlighting the architecture of the cell-based human BBB model. (A) Immunochemistry image of brain tissue showing glial cells and brain endothelial capillaries. (B) Image showing primary glial cells with glial fibrillary acid protein staining. (C) Image showing primary brain endothelial cells stained with anti-CD31 antibody.

Table 1. Selected Marketed Compounds, BBB Transport Mechanism and In Vitro Efflux Ratio Obtained Using the In Vitro Cell-Based Human BBB Model

compounds	therapeutic class	BBB transport mechanism	P_{appAB} ($\times 10^{-6}$ cm^{-1})	P_{appBA} ($\times 10^{-6}$ cm^{-1})	efflux ratio
pravastatine	anticholesteremic agent	active uptake/active efflux[18]	2.3	4.6	2.0
etoposide	antineoplastic agent	passive diffusion/active efflux[19]	1.4	2.8	2.0
digoxin	cardiogoxin	passive difusion/active uptake[20]	3	22.5	7.5
taurocholate	gastrointestinal agent	active uptake/active efflux[21]	2.2	5.4	2.5
vinblastine	antineoplastic agent	passive diffusion/active efflux[22]	2.0	6.0	3.0
propranolol	antihypertensive agent	passive diffusion	40.5	42.2	1.0
haloperidol	antipsychotic agent	passive diffusion	22.0	20	0.9
acetaminophen	analgesic agent	passive diffusion	9.8	8.8	0.9
dextrometorphan	excitatory aminoacid antagoniste	passive diffusion	28.0	42.9	1.5
midazolam	anesthesic	passive diffusion	28.2	41.8	1.5
rosuvastatin	anticholesteremic agent	active uptake/active efflux[20,23]	1.9	1.1	0.6
caffeine	CNS stimulant agent	passive diffusion/active uptake[24]	35.1	37.4	1.0

higher than 35, we considered the expression level too low to be applicable.

For a thorough evaluation of the in vitro BBB model, bidirectional transport experiments were carried out as described above using known transporter substrates (Table 1) in order to ascertain functional activity of transporters across the in vitro cell-based human BBB model. The permeability from the basolateral to apical compartment is P_{appBA}, the permeability from the apical to the basolateral compartment is P_{appAB} and the Q ratio is the efflux ratio as stated in Table 1.

Cell-Based Human Blood−Brain Barrier Model: Integrity and Establishment of Dynamic Range of Permeability. Before use, BBB integrity was checked on 12% of monolayers by sucrose passage. Transwells^R with human BEC monolayers were transferred to new plates. Transport buffer (150 mM NaCl, 5.2 mM KCl, 2.2 mM $CaCl_2$, 0.2 mM $MgCl_2$, 6 mM $NaHCO_3$, 2.8 mM glucose and 5 mM Hepes) was added:

1.5 mL to the basolateral compartment (B) and 0.5 mL to the apical compartment (A) one containing 0.37×10^{10} Bq/mL of [^{14}C]-labeled sucrose. After 60 min of incubation at 37 °C, supernatants from both A and B compartments were collected and the amount of tracer that passed through the endothelial monolayer was determined by scintillation counting. Monolayers were checked for a sucrose permeability from A to B and B to A below to 8×10^{-6} cm s^{-1}.[25]

In order to establish a dynamic range of permeability across the in vitro cell-based human BBB model, known CNS (acetaminophen propranolol, haloperidol, dextrometorphan, midazolam) and non-CNS compounds (digoxin, etoposide, pravastatin, taurocholate, vinblastine, rosuvastatin and caffeine) were used as test probes at concentration 10 μM. The radiolabeled compounds or the nonradiolabeled compounds were introduced in the donor chamber (either the apical or the basolateral compartment). At 60 min, aliquots were removed from the acceptor and donor chambers for determination of drugs' concentrations, and the apparent permeability (P_{app}) values were calculated as previously reported[11] and described below. All experiments were performed in triplicate for each compound.

Analysis of In Vitro BBB Sampling for the Nonradiolabeled Compounds. Acetaminophen, midazolam, rosuvastatine dextrometorphan and caffeine were assayed in vitro BBB media by mean of a LC−MS/MS method. Briefly, in 200 μL of incubation medium, 20 μL of a solution mixture of internal standards (levallorphan, [^{3}D]-glucuronide-acetaminophen and [^{13}C]-1-hydroxymidazolam, meloxicam) were added, and samples were let for 15 min. Finally 20 μL was injected into the chromatographic system made up an Acquity UPLC system coupled to a triple quadrupole mass spectrometer Quattro Premier XE equipped with a turbo spray ionization source (Waters, Saint Quentin en Yvelines, France). System control and data processing were carried out using MassLynx software version 4.1. The chromatographic step was performed on an ACQUITY UPLC BEH Shield RP18 column (2.1 mm ×100 mm, 1.7 μm) coupled with an ACQUITY UPLC BEH Shield RP18 1.7 μmVan Guard Pre-Column (Waters, Saint Quentin en Yvelines, France) set at 50 °C. A gradient of two solvent mixtures was delivered at 0.4 mL/min. Solvent A comprised 0.1% formic acid in water and solvent B, 0.1% formic acid in acetonitrile. Analytes were ionized in either positive or negative (phenacetine) mode. Tuning parameters were capillary voltage 3 kV, source temperature 120 °C, desolvatation temperature 350 °C, desolvatation nitrogen gas 900 L/h, cone gas 10 L/h, collision argon gas flow 0.05 mL/min with a pressure of $2.6.10^{-3}$ bar. Multiple reaction monitoring was used for analytes quantification against internal standards.

Analysis of Permeability Data. The P_{app} value was calculated as follows:

$$P_{app} = dQ/dT \times A \times C_0 \quad (1)$$

where dQ/dT is amount of drug transported per time; A is membrane surface area; C_0 is donor concentration at time 0. Data are presented as the average ± SD from three monolayers. Mass balance of all compounds was set between 80% and 120% as an acceptance criteria. The mass balance was calculated as follows:

$$R\,(\%) = ([(A_p + B_s)/A_0] \times 100 \quad (2)$$

where A_p and B_s are the amount of tested compounds in the apical and basolateral compartments, respectively. A_0 is the initial amount in the donor compartment at time 0.

In Vitro Radioligand-Transport Study Using Cell-Based Human BBB Model. Before the kinetic experiments, the astrocytes were removed from the basolateral compartment and the media from apical and basolateral compartments were replaced by transport buffer (150 mM NaCl, 5.2 mM KCl, 2.2 mM $CaCl_2$, 0.2 mM $MgCl_2$, 6 mM $NaHCO_3$, 2.8 mM glucose and 5 mM Hepes) in both sides. Cells were preincubated with transport buffers for 30 min before drug transport experiments. Experiments were done in triplicate for each compound. The labeled compounds (137 kBq) were introduced in the donor chamber (either apical or basolateral compartment). At time point 30 min after the addition of the radioactive medium, aliquots were removed from the

(17) Bousquet, L.; Pruvost, A.; Guyot, A. C.; Farinotti, R.; Mabondzo, A. Combination of tenofovir and emtricitabine plus efavirenz: in vitro modulation of ABC transporter and intracellular drug accumulation. *Antimicrob. Agents Chemother.* **2009**, *53*, 896–902.
(18) Tsuji, A.; Saheki, A.; Tamai, I.; Terasaki, T. Transport mechanism of 3-hydroxy-3-methylglutaryl coenzyme A reductase inhibitors at the blood−brain barrier. *J. Pharmacol Exp Ther.* **1993**, *267*, 1085–1090.
(19) Kusuhara, H.; Sugiyama, Y. Efflux transport systems for organic anions and cations at the blood-CSF barrier. *Adv. Drug Delivery Rev.* **2004**, *56*, 1741–1763, Review.
(20) Ose, A.; Kusuhara, H.; Endo, C.; Tohyama, K.; Miyajima, M.; Kitamura, S.; Sugiyama, Y. Functional characterization of mouse organic anion transporting peptide 1a4 in the uptake and efflux of drugs across the blood−brain barrier. *Drug Metab. Dispos.* **2010**, *38*, 168–176.
(21) Kitazawa, T.; Terasaki, T.; Suzuki, H.; Kakee, A.; Sugiyama, Y. Efflux of taurocholic acid across the blood−brain barrier: interaction with cyclic peptides. *J. Pharmacol. Exp. Ther.* **1998**, *286*, 890–895.
(22) Miller, D. S.; Nobmann, S. N.; Gutmann, H.; Toeroek, M.; Drewe, I.; Ficker, G. Xenobiotic transport across isolated brain microvessels studied by confocal microscopy. *Mol. Pharmacol.* **2000**, *58*, 1357–1367.
(23) Choi, J. H.; Lee, M. G.; Cho, J. Y.; Lee, J. E.; Kim, K. H.; Park, K. Influence of OATP1B1 genotype on the pharmacokinetics of rosuvastatin in Koreans. *Clin. Pharmacol. Ther.* **2008**, *83*, 251–257.
(24) Potschka, H.; Löscher, W. Multidrug resistance-associated protein is involved in the regulation of extracellular levels of phenytoin in the brain. *NeuroReport* **2001**, *12*, 2387–2389.
(25) Hembury, A.; Mabondzo, A. Endothelin-1 reduces p-glycoprotein transport activity in an in vitro model of human adult blood−brain barrier. *Cell. Mol. Neurobiol.* **2008**, *28*, 915–921.

acceptor chamber for radioactivity counting. The permeability (P_e) was calculated as previously described.[26]

Experimental Setup Using Caco-2 Cell Monolayer. Caco-2 cells (ATCC HTB-37) were maintained in Dulbecco's modified Eagle medium (DMEM) with 10% fetal bovine serum and penicillin (100 units mL^{-1})/streptomycin (100 μg/mL) in 75 cm^2 flasks, with feeding every 2 days. Trypsinized cells were suspended in medium and seeded in BD BioCoat fibrillar collagen 24-multiwell insert systems at 24,500 cells/well in 0.4 mL of medium. The cells were allowed to grow to confluence and differentiate for 21 days, and permeability assays were performed on the 22nd day. Due to the half-life of radiolabeled compounds, we have used the unlabeled compounds for drug transport experiments and an analytical assay was developed. Fifty millimolar stock solutions of test compounds were diluted to 10 μM in transport buffer (Hanks buffered salt solution +10 mM HEPES + 10 mM glucose, pH 7.4). 100 μM Lucifer Yellow was included in the apical side buffer to determine permeability of the monolayer. Control compounds were ranitidine (low permeability control) and warfarin (high permeability control) and were included as internal controls in every study. 0.25 mL of compound solution was added to the apical compartment or 1.0 mL to the basolateral compartment with buffer on the other side of the monolayer, and incubated for 120 min at 37 °C. At the end of the 120 min incubation period the compounds were harvested from both sides of the monolayer and the amount of compound was determined by LC/MS analysis. The integrity of the monolayers was established by measuring Lucifer Yellow permeability ($P_{app} = 8 \times 10^{-7}$ cm s^{-1}).

In Vivo Plasma−Brain Exchange Parameters: K_1 and k_2. The in vivo plasma−brain exchange parameters used for comparison to in vitro data were determined previously in humans by PET using a kinetic analysis of the radiotracer binding. For each radiotracer, the parameters were determined by fitting the brain kinetics of the radiotracer using a two- or three-tissue compartment model of the ligand−receptor interaction.

This model includes the free unmetabolized ligand in plasma (denoted C_p) and three tissue compartments, namely, free ligand in the tissue (M_f), ligand specifically bound to receptor sites (M_b) and nonspecific binding (M_{ns}) (Figure 2); and seven parameters, namely, the binding site concentration (B'_{max}) and six kinetic parameters describing the kinetics between the compartments (K_1, k_2, k_3, k_4, k_5, and k_6). The nonspecific binding compartment can be summed together with the free compartment when they are known to be at equilibrium.

The multi-injection approach was developed to allow determination of the receptor density B_{max} and the affinity K_d.[27] It is based on the injections of non-negligible amount

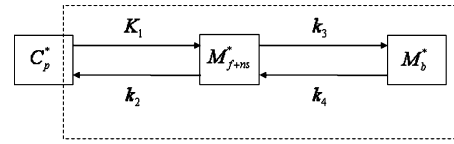

$$k_3 = k_{on}/V_R \cdot \left(B'_{max} - M_b^*\right)$$
$$k_4 = k_{off}$$
$$K_d V_R = \frac{k_{off}}{k_{on}/V_R}$$

Figure 2. Compartmental schematic describing the brain drug efflux transport kinetic. The measured arterial plasma concentration of the unmetabolized radioligand is denoted as $C_p^*(t)$. The flux of radioligand from the arterial plasma compartment to the free compartment is given by $K_1 C_p^*(t)$. The quantity of free radioligand present in 1 mL of the tissue volume is denoted by $M_f^*(t)$. The free ligand can escape back to the blood circulation with a rate constant k_2, or bind to an unoccupied specific receptor site with a rate constant k_3. $M_b^*(t)$ is the quantity of receptors sites in 1 mL of tissue already occupied by the radioligand. The rate constant for the dissociation of the specifically bound ligand is denoted by k_4. In the multiinjection protocols the specific binding is a saturable reaction that depends on the bimolecular association rate constant k_{on}, the free ligand concentration in the vicinity of the receptors sites $M_f^*(t)$, and the quantity of free receptors in 1 mL of tissue. This last quantity is equal to $B'_{max} - M_b^*(t)$. Thus using the multi-injection protocol $k_3 = (B'_{max} - M_b^*(t))$. B'_{max} is the total receptor site concentration available for binding.The simulated PET data (denoted as $M_{TEP}^*(t)$) corresponding to the PET scan performed between time t_i and t_{i+1} is given by the following equation:

$$M_{TEP}^*(t_i) = \frac{1}{t_{i+1} - t_i} \int_{t_i}^{t_{i+1}} (M_f^*(t) + M_b^*(t) + F_V C_b^*(t))\, dt$$

where $C_b^*(t)$ is the whole blood time−concentration curve and where F_V represents the fraction of blood present in the tissue volume.

of unlabeled ligand, in order to partially saturate the binding sites. Thus, at this time, the tracer conditions are no more considered, and the k_3 parameter is no longer linear, but depends on the fraction of binding sites occupied:

$$k_3 = k_{on}(B_{max} - M_b) \quad (3)$$

This methodology allows the determination of the receptor density B_{max} and the affinity:

$$K_d = k_{on}/k_{off} \quad (4)$$

where k_{off} is k_4.

Detailed descriptions and discussions of this procedure have been published previously.[28]

The multi-injection protocol was used for the determination of the parameter for [^{11}C]flumazenil in baboon[29] and in human,[30] for [^{11}C]befloxatone in baboon[31] and in human (manuscript in preparation) and for [^{11}C]raclopride.[29] For [^{18}F]fluoro-A-85380, the multi-injection was used in ba-

(26) Pardridge, W. M.; Triguero, D.; Yang, J.; Cancilla, P. A. Comparison of in vitro and in vivo models of drug transcytosis through the blood−brain barrier. *J. Pharmacol. Exp. Ther.* **1990**, *253*, 884–891.

boon[28] and a linear 2TC in human.[32] [^{18}F]-FDG and [^{18}F]-FDOPA parameters were determined using a linear 2TC model, without k_4, because they are considered irreversible.[33,34] In the model used, the kinetic rate constant of the free ligand from the plasma to the free ligand compartment in the brain is denoted K_1, while k_2 represents the kinetic rate constant of the free ligand in the brain that escapes back to the blood circulation.

Since the two-compartmental model used here includes a specific binding compartment, the K_1 and k_2 parameters are independent of the brain accumulation of the radiotracer on the receptors. Thus, K_1 and k_2 represent the rate of the radiotracer exchanged with the brain and can be compared to $P_{e\text{-}AB}$ and $P_{e\text{-}BA}$ as measured in vitro as we reported previously.[11]

Statistical Analysis. Statistical analysis was performed using the Prism 3.0 program (GraphPad Software, Inc., San Diego, CA). Statistical comparisons conducted herein were accomplished using the two tailed nonparametric Pearson test for regression lines. Changes were considered statistically significant at $P < 0.05$.

Results

In Vitro Cell-Based-Human BBB Model. *Integrity of the In Vitro Cell-Based Human BBB Model.* Before permeation screening of [^{18}F] or [^{11}C]-labeled compounds, the integrity of the in vitro system was evaluated to establish the suitability of this model as a permeability tool. The sucrose penetration in the acceptor compartment of the in vitro cell-based human BBB model was low. The mean P_{app} value from 9 different batches of 9 different donors was $2.69 \times 10^{-6} \pm 0.25$ cm s^{-1} (CV: 23.28%) indicating a restrictive transport of sucrose, a paracellular marker, across the in vitro cell-based human BBB and thus confirmed a well-formed cell monolayer with acceptable monolayer integrity. This integrity was associated with the expression between neighboring endothelial cells of claudin-3, claudin-5 and ZO-1 mRNA expression (Figure 3A). The in vitro cell-based human BBB model shows mRNA expression of glucose transporter 1 (SLC2A1), amino acid transporters (LAT1 and LAT2) and efflux transporters (Figure 3B and 3C). In contrast to ABCG2, ABCB1, ABCC4, ABCC5 and ABCC, neither ABCC2 nor ABCC6 mRNA transcripts were detected in the in vitro cell-based human BBB model (Figure 3C).

Dynamic Range of Permeability and Polarity of In Vitro Cell-Based Human BBB Model. To establish a dynamic range of permeability across the in vitro cell-based human BBB model, the permeability of CNS and non-CNS compounds was evaluated. The mean P_{app} value for the marketed non-CNS compounds from the apical to basolateral compartment ranges from $1.40 \pm 0.5 \times 10^{-6}$ cm s^{-1} to $3 \pm 0.008 \times 10^{-6}$ cm s^{-1}, consistent with a limited passage across the human brain endothelial cell monolayer. The permeability value for CNS compounds such as midazolam, propranolol, dextrometorphan and haloperidol, consistent with high passive apparent permeability, ranges from $9.79 \pm 0.90 \times 10^{-6}$ cm s^{-1} to $35.80 \pm 2.38 \times 10^{-6}$ cm s^{-1} (Figure 4). To demonstrate the polarity of human BBB active efflux transporters, bidirectional transport experiments with known efflux transporters' substrates were performed, as previously reported.[25,35] Then, the permeability from the basolateral to apical compartment and from the apical to the basolateral compartment (Q ratio) was calculated. Compounds that display efflux ratio at least twice that of influx (Q ratio ≥ 2) are considered to be subject to effective efflux, and compounds that display efflux less than or equal to the influx (Q ratio below or close to 1) are considered to be transported by passive diffusion or undergo an effective influx.[11] Effective efflux implies the involvement of an active transporter. All tested non-CNS compounds exhibited $Q \geq 2$ (Table 1), suggesting the involvement an effective efflux transporter at the level of the in vitro cell-based human BBB model. These data are in agreement with the observations of ABCB1, ABCG2, ABCC1, ABCC4, ABCC5 at the level of in vitro human

(27) Delforge, J.; Syrota, A.; Bottlaender, M.; Varastet, M.; Loc'h, C.; Bendriem, B.; Crouzel, C.; Brouillet, E.; Maziere, M. Modeling analysis of [11C]flumazenil kinetics studied by PET: application to a critical study of the equilibrium approaches. *J. Cereb. Blood Flow Metab.* **1993**, *13*, 454–468.

(28) Gallezot, J. D.; Bottlaender, M.; Delforge, J.; Valette, H.; Saba, W.; Dolle, F.; Coulon, C.; Ottaviani, M.; Hinnen, F.; Syrota, A.; Gregoire, M. C. Quantification of cerebral nicotinic acetylcholine receptors by PET using 2-[^{18}F]fluoro-A-85380 and the multiinjection approach. *J. Cereb. Blood Flow Metab.* **2008**, *28*, 172–189.

(29) Pappata, S.; Dehaene, S.; Poline, J. B.; Gregoire, M. C.; Jobert, A.; Delforge, J.; Frouin, V.; Bottlaender, M.; Dolle, F.; Di Giamberardino, L.; Syrota, A. In vivo detection of striatal dopamine release during reward: a PET study with [11C]raclopride and a single dynamic scan approach. *NeuroImage* **2002**, *16*, 1015–1027.

(30) Delforge, J.; Pappata, S.; Millet, P.; Samson, Y.; Bendriem, B.; Jobert, A.; Crouzel, C.; Syrota, A. Quantification of benzodiazepine receptors in human brain using PET, [^{11}C]flumazenil, and a single-experiment protocol. *J. Cereb. Blood Flow Metab.* **1995**, *15*, 284–300.

(31) Bottlaender, M.; Valette, H.; Delforge, J.; Guenther, I.; Saba, W.; Dollé, F.; Curet, O.; George, P.; Grégoire, M.-C. In vivo Quantification of Monoamine Oxidase-A in baboon brain: A PET study using [^{11}C]befloxatone and the multi-injection approach. *J. Cereb. Blood Flow Metab.* **2010**, *30*, 792–800.

(32) Gallezot, J. D.; Bottlaender, M.; Grégoire, M. C.; Roumenov, D.; Deverre, J. R.; Coulon, C.; Ottaviani, M.; Dollé, F.; Syrota, A.; Valette, H. In vivo imaging of human cerebral nicotinic acetylcholine receptors with 2-18F-fluoro-A85830 and PET. *J. Nucl. Med.* **2005**, *46*, 240–247.

(33) Huang, S. C.; Yu, D. C.; Barrio, J. R.; Grafton, S.; Melega, W. P.; Hoffman, J. M.; Satyamurthy, N.; Mazziotta, J. C.; Phelps, M. E. Kinetics and modeling of L-6-[18F]fluoro-dopa in human positron emission tomographic studies. *J. Cereb. Blood Flow Metab.* **1991**, *11*, 898–913.

(34) Heiss, W. D.; Pawlik, G.; Herholz, K.; Wagner, R.; Göldner, H.; Wienhard, K. Regional kinetic constants and cerebral metabolic rate for glucose in normal human volunteers determined by dynamic positron emission tomography of [18F]-2-fluoro-2deoxy-D-glucose. *J. Cereb. Blood Flow Metab.* **1984**, *4*, 212–23.

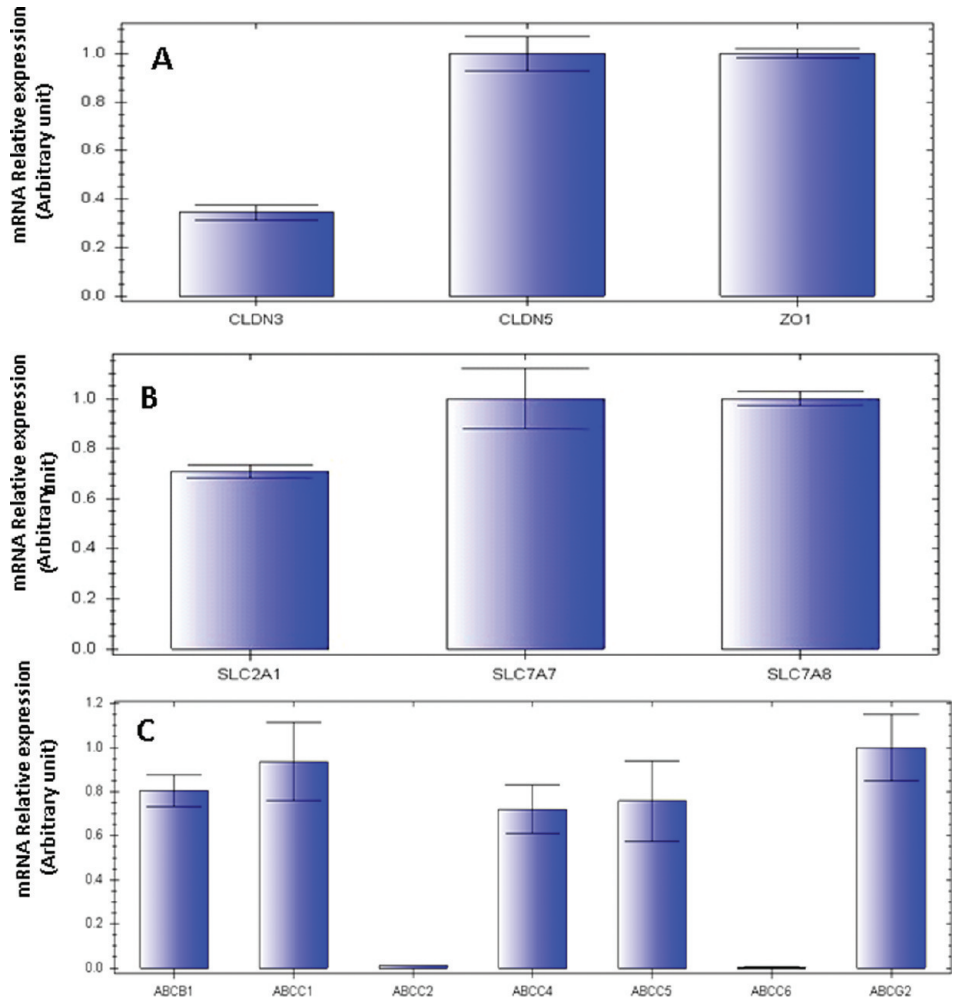

Figure 3. mRNA profile expression of tight junction and transporter in the cell-based human BBB model: (A) mRNA expression of ZO-1, claudin 3 and Claudin 5; (B) mRNA expression of glucose transporter 1 (SLC2A1), LAT1 and LAT2 transporters; (c) mRNA expression of seven ATP-binding cassette (ABC) in cell-based human BBB model. Results are means from 3 patients of 3 independent experiments.

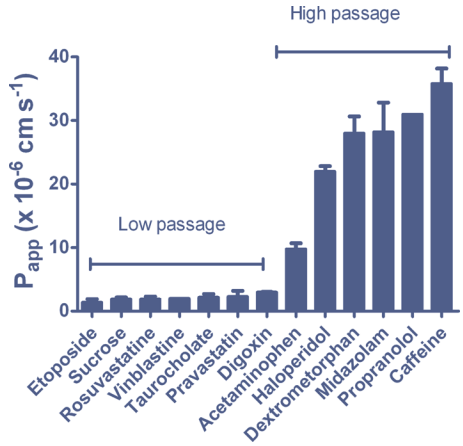

Figure 4. Distribution of permeability (P_{app}) values for selected CNS versus non CNS compounds. Each data represents the mean ± SD of three cell monolayers.

BBB (Figure 3C). Moreover, the level of mRNA ABC transporters and more specifically ABCB1 and ABCG2 is comparable to the level of freshly isolated brain microvessels.[36]

Table 2. In Vivo K_1, k_2, DV, and In Vitro $P_{e\text{-}AB}$, $P_{e\text{-}BA}$ and Q ($P_{e\text{-}AB}/P_{e\text{-}BA}$) Ratio of 7 Compounds Studied

compounds	in vivo K_1, mL cm^3 min^{-1}	in vivo k_2, min^{-1}	DV, mL cm^{-3}	in vitro $P_{e\text{-}AB}/P_{e\text{-}BA}$
befloxatone	0.2	0.24	0.83	3.41
fluorodopa	0.03	0.04	0.75	3.25
FDG	0.09	0.13	0.69	1.90
flumazenil	0.35	0.57	0.61	1.15
fluoro-A-85380	0.11	0.45	0.24	0.13
raclopride	0.09	0.45	0.2	0.07
PE2I	nd[a]	nd	nd	0.66

[a] Not determined.

In Vivo versus In Vitro Studies. Human PET images acquired over 1 min after intravenous injection of radiolabeled compounds (Table 2) discriminate the compounds with moderate/high and low cerebral uptake. For instance, a typical representation for [^{11}C]befloxatone and 2-[^{18}F]fluoro-A-85380 is shown in Figure 5A. At this early time point, a cerebral uptake of [^{11}C]befloxatone was higher than for [^{18}F]fluoro-A-85380. Figure 5B shows the corresponding percentage of injected dose taken per milliliter of brain and

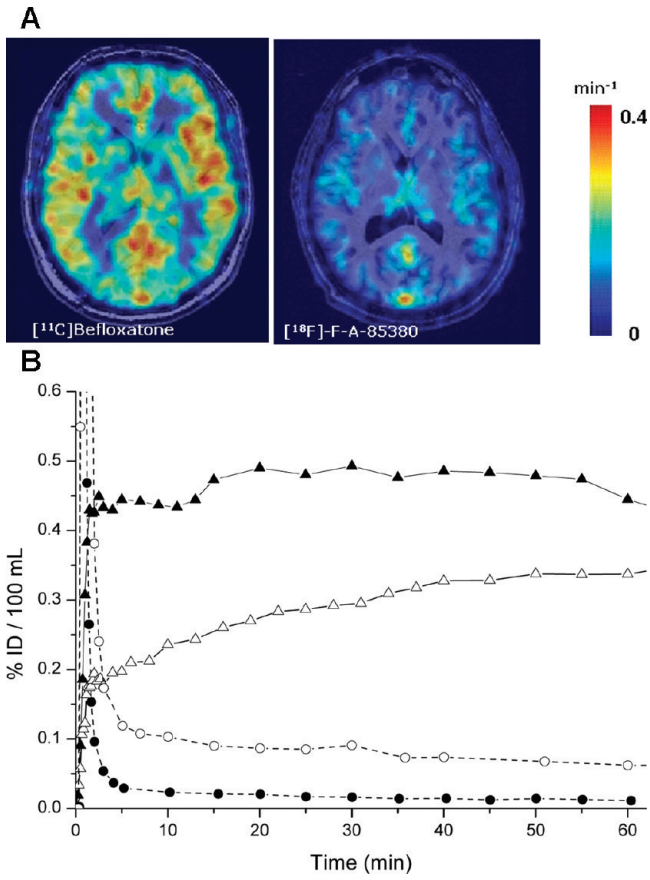

Figure 5. In vivo versus in vitro cell-based human BBB permeability studies. (A) Typical imaging data. Coregistered PET-MRI images representing the K_1 obtained in human after intravenous injection of [^{11}C]befloxatone (left) and [^{18}F]fluoro-A-85380 (right). The PET images representing the K_1 are obtained as follows. PET image obtained at 1 min post injection (mean value between 30 and 90 s) is considered as independent of the receptor binding. This image (in Bq/mL) is corrected from the vascular fraction (F_v in Bq/mL, considered as 4% of the total blood concentration at 1 min) and divided by the arterial plasma input function (AUC0−1 min of the plasma concentration, in (Bq min)/mL). The resulting parametric image, expressed in min^{-1}, represents an index of the K_1 parameter of the radiotracer. (B) Time−activity curves obtained in the thalamus (triangles, solid lines) and in plasma (circles, dashed lines) in healthy volunteer after iv administration of [^{18}F]fluoro-A-85380 (open symbols) or [^{11}C]befloxatone (closed symbols).

plasma from 1 to 60 min after intravenous injection. The compound [^{18}F]fluoro-A-85380 showed an early and low cerebral peak compared to [^{11}C]befloxatone compound. Then the cerebral uptake increased to a plateau reached at 40−60 min postinjection for both compounds. The pharmacokinetics of the BBB passage was analyzed according to a two-compartmental model (arterial blood and brain tissue), separated by the BBB (Figure 2). The in vivo cerebral and whole blood kinetics were analyzed according to this model and the influx rate constant (K_1), and the flux rate constant (k_2). The K_1 and k_2 parameters did not take into account the brain accumulation of the radiotracer on the receptors. Thus, K_1 and k_2 represent the rate of the radiotracer exchanged through the BBB and can be compared to $P_{e\text{-}AB}$ and $P_{e\text{-}BA}$ as measured in vitro using cell-based human BBB model.

The K_1/k_2 ratio according to a two-tissue compartment model was about 0.83 for [^{11}C]befloxatone (unpublished lab data), 0.69 for [^{18}F]FDG,[23] 0.61 for [^{11}C]flumazenil,[30] 0.24 for 2-[^{18}F]fluoro-A-85380,[32] 0.75 for[^{18}F]-FDOPA and 0.20 for [^{11}C]raclopride.[29] The K_1/k_2 ratio for PE2I was not determined.

The in vitro permeability of [^{18}F] and [^{11}C] compounds was measured from the apical to basolateral compartment ($P_{e\text{-}AB}$) and vice versa ($P_{e\text{-}BA}$), and the $P_{e\text{-}AB}/P_{e\text{-}BA}$ ratio was calculated. 2-[^{18}F]Fluoro-A-85380 and [^{11}C]raclopride show limited passage. These compounds showed a low K_1/k_2 ratio (below 0.3) corresponding to a low cerebral uptake (Figure 5A). Conversely, high in vitro BBB permeability was observed for [^{11}C]flumazenil, [^{11}C]befloxatone, [^{18}F]-FDOPA, and [^{18}F]-FDG. For these compounds, PET analysis demonstrated a cerebral uptake ($K_1/k_2 > 0.6$). The in vitro ratio $P_{e\text{-}AB}/P_{e\text{-}BA}$ showed a highly significant correlation with the in vivo distribution volume of tested compounds in human ($r^2 = 0.90$; $P < 0.001$) (Figure 6A). The in vivo pharmacokinetic parameters of the same PET tracers were compared to the traditional permeability tool, Caco-2 cells. No correlation was observed between human brain penetration and in vitro Caco-2 permeability ($r^2 = 0.17$, Figure 6B).

Discussion

Many new drugs designed to work in the CNS may show exceptional therapeutic promise due to their high potency at the receptor or target site and in vitro binding assays, but lack general efficacy when administered systemically. In many cases, the problem is due to lack of penetration of the BBB, and this has become a major problem that has impeded the discovery and development of active CNS drugs. We previously reported the development of a new coculture-based model of human BBB able to predict passive and active transport of molecules into the CNS.[4,11] The present work reports for the first time the evaluation of the BBB permeabilities of a series of compounds studied correlatively in vitro using a human BBB model and in vivo with quantitative PET imaging in the clinic.

Collectively, our findings indicate that the in vitro coculture model of human BBB has important features of the BBB

(35) Bousquet, L.; Roucairol, C.; Hembury, A.; Nevers, M. C.; Creminon, C.; Farinotti, R.; Mabondzo, A. Comparison of ABC transporter modulation by atazanavir in lymphocytes and human brain endothelial cells: ABC transporters are involved in the atazanavir-limited passage across an in vitro human model of the blood−brain barrier. *AIDS Res. Hum. Retroviruses* **2008**, *24*, 1147–1154.

(36) Dauchy, S.; Dutheil, F.; Weaver, R. J.; Chassoux, F.; Daumas-Duport, C.; Couraud, P. O.; Scherrmann, J. M.; De Waziers, I.; Declèves, X. ABC transporters, cytochromes P450 and their main transcription factors: expression at the human blood−brain barrier. *J. Neurochem.* **2008**, *107*, 1518–28.

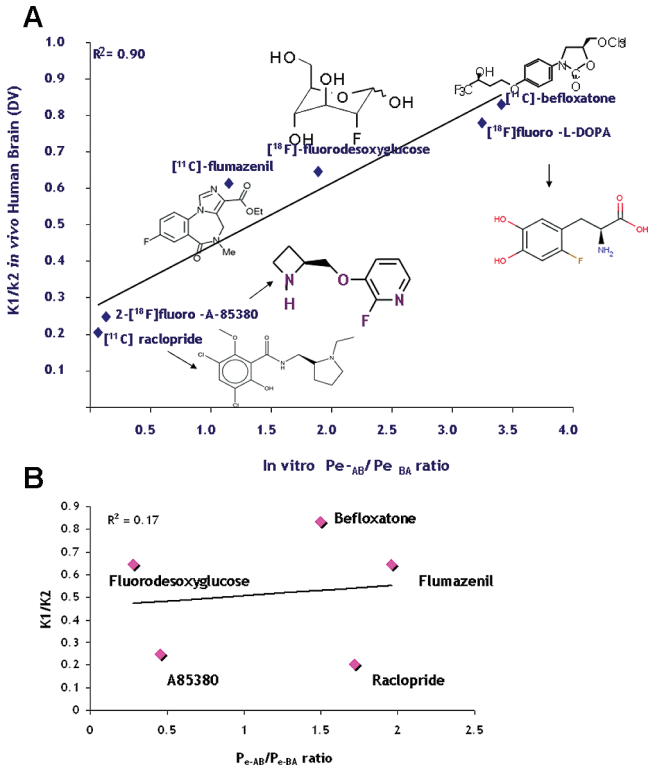

Figure 6. (A) Graph showing the relationship between the K_1/k_2 ratio and the in vitro $P_{e\text{-}AB}/P_{e\text{-}BA}$ ratio using the cell-based human BBB model. Regression line was calculated, and correlation was estimated by the two-tailed nonparametric Spearman test. (B) Graph showing the relationship between the K_1/k_2 ratio and the in vitro $P_{e\text{-}AB}/P_{e\text{-}BA}$ ratio using Caco-2 cell monolayer.

in vivo (low paracellular permeation, well-developed tight junctions, functional expression of efflux transporters) and is suitable for discriminating between CNS and non-CNS compounds. It has long been recognized that it is important to cross-correlate in vitro and in vivo pharmacokinetic data in order to validate experimental models and to assess the predictive power of the techniques,[26] and appropriate correlation studies were performed to establish that. It is generally accepted that it is the unbound drug that exerts the physiological effect. Literature reports highlight the prime importance of drug concentration in brain and plasma tissues for cross-correlating in vitro and in vivo pharmacokinetic data.[37−39] Drug concentration and essentially free drug concentration in the brain seem to provide the most important link with pharmacological action.[37] Differential binding of compounds in plasma or brain tissue can overwhelm the apparent permeability of compounds. In this view, in vivo PET approach used for validation of in vitro cell-BBB model is one of the latest technologies taking into account these considerations.[37−39] PET imaging is the advanced technology to obtain biochemical information such as blood flow, distribution of receptors and P-gp transport activity in vivo.[40] Thus it allows monitoring of the whole pharmacokinetic time course in physiological conditions. Brain kinetics can be analyzed by compartmental modeling or graphical evaluation, which allows the calculation of the BBB PS permeability.[41−43] In the present study, using PET imaging and the two-compartmental model for calculation of pharmacokinetic parameters, we avoid the binding properties of compound to the brain or plasma tissue. Thus, PET imaging can measure with accuracy the kinetic rate constant of the free ligand from the plasma to the free ligand compartment in the brain (K_1) and the kinetic rate constant of the free ligand in the brain that escapes back to the blood circulation (k_2). In vivo cerebral pharmacokinetics supplies global information on the degree and the rate of BBB passage. Our PET approach is consistent with the new concept of CNS drug penetration described elsewhere.[35]

Taking into account these considerations, we evaluated drug permeation into the human brain using PET imaging in parallel to the assessment of drug permeability across the in vitro model of the human BBB and across the Caco-2 cell monolayer. Caco-2 cells, a human colon adenocarcinoma, undergo spontaneous enterocytic differentiation in culture and become polarized cells with well-established tight junctions, resembling intestinal epithelium in humans. It has also been demonstrated that the permeability of drugs across Caco-2 cell monolayers correlates very well with the extent of oral absorption in humans. In the past 10 to 15 years, the Caco-2 cells have been widely used as an in vitro tool for evaluating the intestinal permeability property of discovery

(37) Summerfield, S. G.; Read, K.; Begley, D. J.; Obradovic, T.; Hidalgo, I. J.; Coggon, S.; Lewis, A. V.; Porter, R. A.; Jeffrey, P. Central nervous system drug disposition: the relationship between in situ brain permeability and brain free fraction. *J. Pharmacol. Exp. Ther.* **2007**, *322*, 205–213.

(38) Liu, X.; Smith, B. J.; Chen, C.; Callegari, E.; Becker, S. L.; Chen, X.; Cianfrogna, J.; Doran, A. C.; Doran, S. D.; Gibbs, J. P.; Hosea, N.; Liu, J.; Nelson, F. R.; Szewc, M. A.; Van, D. J. Use of a physiologically based pharmacokinetic model to study the time to reach brain equilibrium: an experimental analysis of the role of blood−brain barrier permeability, plasma protein binding, and brain tissue binding. *J. Pharmacol. Exp. Ther.* **2005**, *313*, 1254–1262.

(39) Wan, H.; Ahman, M.; Holmen, A. G. Relationship between brain tissue partitioning and microemulsion retention factors of CNS drugs. *J. Med. Chem.* **2009**, *52*, 16931700.23. Hurko, O.; Ryan, J. L. Translational research in central nervous system drug discovery. *NeuroRx* **2005**, *2*, 671–682.

(40) Syvänen, S.; Lindhe, O.; Palner, M.; Kornum, B. R.; Rahman, O.; Långström, B.; Knudsen, G. M.; Hammarlund-Udenaes, M. Species differences in blood−brain barrier transport of three positron emission tomography radioligands with emphasis on P-glycoprotein transport. *Drug Metab. Dispos.* **2009**, *37*, 635–643.

(41) Guo, Q.; Brady, M.; Gunn, R. A biomathematical model approach to central nervous system radioligand discovery and development. *J. Nucl. Med.* **2009**, *50*, 1715–1723.

(42) Liu, X.; Tu, M.; Kelly, R. S.; Chen, C.; Smith, B. J. Development of a computational approach to predict blood−brain barrier permeability. *Drug Metab. Dispos.* **2004**, *32*, 132–139.

(43) Hammarlund-Udenaes, M.; Fridén, M.; Syvänen, S.; Gupta, A. On the rate and extent of drug delivery to the brain. *Pharm. Res.* **2008**, *258*, 1737–1750. Review.

compounds and is sometimes used as an in vitro alternative for providing initial insights into BBB permeability of leads.[44,45]

2-[^{18}F]Fluoro-A-85380 and [^{11}C]raclopride show absent or low cerebral uptake with the K_1/k_2 ratio under 0.3, while [^{11}C]flumazenil, [^{11}C]befloxatone and [^{18}F]-FDG and FDOPA show a cerebral uptake with the K_1/k_2 ratio above 0.6. FDOPA and FDG uptake is consistent with the fact that these two PET tracers are ligand of amino acid and glucose transporters, respectively. mRNA transcription profile of those receptors was evidenced in the cell-based human BBB model. The in vitro human BBB model discriminates the compounds in the same way as in vivo human brain PET imaging analysis (Figure 6A). However, the in vitro Caco-2 permeability does not correlate with the in vivo brain penetration for tracer, suggesting that it is an unsuitable model for in vivo BBB prediction (Figure 6B). The fact that Caco-2 is a cell line could influence drug permeability. ABCC2 is highly expressed in Caco-2 cells (data not shown) while this transporter was not detected in our in vitro BBB model. Data support the concept that the intestinal mucosa and the BBB are different biologic barriers in term of lipid composition and drug-efflux transporter expression.

We demonstrate here a strong correlation between in vitro cell-based human BBB model and in vivo pharmacokinetic data ($r^2 = 0.90$, $P < 0.001$).

In conclusion, this first study demonstrates, despite the small number of radioligands ($n = 6$), a close relationship between the assessment of in vitro human BBB passage and in vivo human brain penetration in human subjects. This in vitro cell-based human BBB model is amenable to high-throughput applications in drug discovery and demonstrates its potential as an effective screening tool for CNS programs. These findings which can be extended to peptides, proteins, viruses and with substances with high degrees of protein binding in vivo or other non-BBB factors dictating their penetration need to be specifically studied. The in vitro BBB model addresses a severe "scientific gap" that exists currently in the screening and selection of compounds for CNS targets. Due to the lack of a good predictive tool, the most common approach involves a combination of in silico, in vivo and in vitro approaches to predict brain penetration. These normally include PAMPA, efflux ratio in Caco-2, and protein-binding properties to assess brain entry or resource-intensive in vivo brain-to-plasma ratio assessment in rodent models. These models either are not fully validated or are very time-, cost- and resource-intensive. This creates a need for more appropriate screening methods that are predictive of the in vivo behavior of drugs in humans and which are relatively low cost and amenable to medium-throughput application in early/mid stage drug discovery programs. Therefore, the in vitro BBB model discussed in this paper presents an attractive tool that strikes a good balance between speed (amenable for handling 10s of compounds per week), cost (cell culture), and resources (manageable via 1−2 FTE's) making it suitable for discovery/development laboratories. The in vitro human BBB model may help to test large numbers of compounds of pharmaceutical importance for CNS diseases and provide a valuable tool to enhance the efficiency as well as effectiveness of CNS discovery organizations.

Acknowledgment. We thank cyclotron and the radiochemistry staff of the Service Hospitalier Fréderic Joliot, France. This work was supported by recurrent funds from the Commissariat à l'Energie Atomique (CEA).

MP1002366

(44) Kerns, E.; Di, L.; Petsky, S.; Farris, M.; Ley, R.; Jupp, P. Combined application of PAMPA and Caco-2 permeability assays in drug discovery. *J. Pharm. Sci.* **2004**, *93* (6), 1440–1453.

(45) Balimane, P. V.; Han, Y. H.; Chong, S. Current industrial practices of assessing permeability and P-gp interaction. *AAPS J.* **2006**, *8* (1), E1−13.